

Subsynchronous torque interaction for HVDC Light B

– a theoretical description

Electrical Engineering

Industrial

Povilas Zizliauskas

M.Sc. thesis

Department of Industrial Electrical Engineering and Automation
Lund University



Summary

Subsynchronous torque interaction (SSTI) is a well known phenomenon in high voltage AC networks. It can be sustained and amplified in power systems with series compensated lines or active devices for power flow or voltage control. These devices introduce negative damping for the turbine-generator system critical frequencies. It is known that also a high voltage direct current (HVDC) link may have a similar effect particularly when connected near a turbine generator as the only load.

In order to identify the risk of interaction in an HVDC project, an SSTI screening study is always performed. If the screening study indicates a potential risk for SSTI oscillations, a more detailed SSTI study is performed, and, if necessary, an SSTI damping controller has to be adapted and integrated in the HVDC control system.

The new technology HVDC Light, HVDC transmission system that includes voltage source converters, does not yet have any established method to assess and perform SSTI studies. This report describes an investigation for determining the physical nature of potential interaction and for determining the first steps to take in order to develop a method for assessing and studying SSTI on HVDC Light.

For the future verification of the methodology and other study purposes, it was decided to develop a Real Time Analogue Simulator (RTAS) for HVDC Light_B. An HVDC Light_B transmission includes three level voltage source converters. The main reason to develop the RTAS was its ability to attain the results of simulation in real time, since digital simulations require integration time steps in the range of some microseconds and thus extensive computer capacity.

The intention of this Master Thesis project was to initiate the investigation of SSTI for HVDC Light_B, and to develop and test out the RTAS for establishing in the future a reliable methodology.

The report describes the work done by Povilas Zizliauskas. Performing this extensive work was his Master thesis project. The work was done at *ABB Power Systems AB* in Ludvika, at the Department for System Simulation, LST. Supervisor for the examination work was Hugo Duch n.

Table of Contents

1	Background	3
1.1	Subsynchronous torsional interaction (SSTI).....	4
1.2	HVDC.....	4
1.2.1	HVDC Classic	5
1.2.2	HVDC Light	6
2	Problem description and investigation approach	8
2.1	Problem description.....	8
2.2	SSTI study	8
2.3	Details of HVDC Light_B	8
2.4	SSTI in HVDC Light_B.....	8
2.5	RTAS set-up.....	8
3	SSTI related to HVDC Classic	9
3.1	Interaction mechanisms.....	9
3.2	Screening study.....	12
3.3	Detailed study	13
3.4	SSDC.....	13
4	HVDC Light _B fundamentals	14
4.1	The three level converter bridge.....	16
4.2	The control system of VSC	20
5	SSTI in HVDC Light	22
6	Converter control impact on SSTI in HVDC Light	24
7	Summary.....	26
7.1	Conclusions/suggestions for verification.....	26
7.2	Recommended continuation	27
8	References.....	28
9	Abbreviations	29
10	Acknowledgements	30
11	Enclosures.....	31
11.1	Enclosure 1: Preliminary studies of SSTI in HVDC Light [5]	31
11.2	Enclosure 2: RTAS set-up	34

1 Background

HVDC is an efficient method to transfer large amounts of electrical power and is used at many places all around the world. The method is very flexible and can be used to transfer electrical power over very long distances both with overhead lines and with cables in water or underground. HVDC is also used to link asynchronous AC networks. Until recently thyristors were used for conversion from AC to DC and vice versa.

Today a new type of HVDC is gaining ground. It makes use of the latest developed semiconductor technology for power conversion between AC and DC. The semiconductors used are IGBTs (Insulated Gate Bipolar Transistors), the converters are VSC (Voltage Source Converters) and they operate with very high frequency (1- 2 kHz) utilising PWM (Pulse Width Modulation). It also utilises a new developed cable for DC power transmission. This technology is known today within ABB under the name of HVDC Light.

HVDC Light_B technology is a new converter scheme configuration, which allows having three states of converter connection: plus, minus and zero (ground potential). This configuration is also called Three Level Converter or Neutral Point Clamped (NPC) Converter.

The phenomenon of subsynchronous torque interaction, arising from an HVDC Light system being connected close to generation units needs to be throughout investigated. Risk for SSTI is investigated today using methods developed for classic HVDC, but the mechanism of interaction for HVDC Light has not been studied in detail. At the initial stage of investigation there were some ideas, pointing out that the nature of such interaction would be different from the same processes in conventional HVDC. The first investigation steps were made using digital models, but a theoretical approach was not done.

The RTAS is an analogue simulator where physical plant control systems operate against a scaled analogue network representation. The network representation includes the most important parts of the transmission system, everything from generators and converters to the DC cables and transformers. The study is made in real time. Analogue real time simulation takes long time to prepare, but on the other hand there is a great amount of time to gain in the actual simulation. This was the method used to accomplish SSTI studies for the HVDC Classic technology before digital simulation in EMTDC was introduced. To perform studies in EMTDC for HVDC Light takes very long time, therefore it would be useful to develop a similar study methodology for HVDC Light_B. RTAS can be implemented using experience from previous projects, and later can be used for verification of new digital models and for specific studies.

1.1 Subsynchronous torsional interaction (SSTI)

Torsional interaction occurs when the induced subsynchronous torque in the generator is close to one of the torsional natural modes of the turbine-generator shaft. When this happens, generator rotor oscillations will build up and this motion will induce armature voltage components at subsynchronous frequencies. Moreover, the phase of this induced subsynchronous frequency voltage is such that it sustains the subsynchronous torque. If this torque equals or exceeds the inherent mechanical damping of the rotating system, the system will become self-excited. This phenomenon is called torsional interaction and occurs in the frequency range of 10-40 Hz.

The most common example of the natural mode subsynchronous oscillation is found in networks that include series capacitor compensated transmission lines or at the rectifier side of an HVDC transmission. When connecting the rectifier side of an HVDC transmission link to an AC network with a turbo generator, the rectifier contributes with negative damping in the subsynchronous frequency range. Depending on the AC network configuration, this may increase the risk of SSTI in the generator system.

Hydro generator systems are not SSTI sensitive when connected to an HVDC transmission link. This is due to the fact that the mechanical damping for possible subsynchronous torsional frequencies is considerably high, and also because the natural torsion frequencies are at higher frequencies compared with thermal generators.

1.2 HVDC

HVDC stands for High Voltage Direct Current and is today a well proven technology employed for power transmission all over the world. The method is very flexible and can be used to transfer electrical power over long distances. Both with power lines on land or with cable in water.

One of the typical HVDC applications is its utilization to transmit electrical power over long distances. Therefore, the two converter stations are to be used: one rectifier and one inverter. Electrical power is taken from one point in an AC network and converted to DC with the help of the rectifier station. The DC power is transmitted by overhead lines or by submarine cables, converted back to AC power at the inverter station and finally injected into the receiving AC network. Other important apparatuses in an HVDC station are the power transformers, smoothing reactor and filters on both AC and DC side. Figure 1.1 shows a basic set up for a classic HVDC application.

The final decision to choose HVDC instead of conventional AC transmissions depends on a number of factors and the main reason often changes between different projects. Some advantages with HVDC compared to HVAC are the following:

- The controllability of the power flow will increase. Both the power direction and the power level can be controlled very accurate and rapidly.
- An HVDC transmission line has lower losses than AC lines for the same power capacity. The losses in the converter stations have of course to be added, but above a certain break-even distance, the total HVDC transmission losses become lower than the AC losses. HVDC cables also have lower losses than AC cables.
- For long submarine cable links HVDC is the only possible technical solution.

- When connecting two asynchronous AC networks together, an HVDC link has to be implemented.

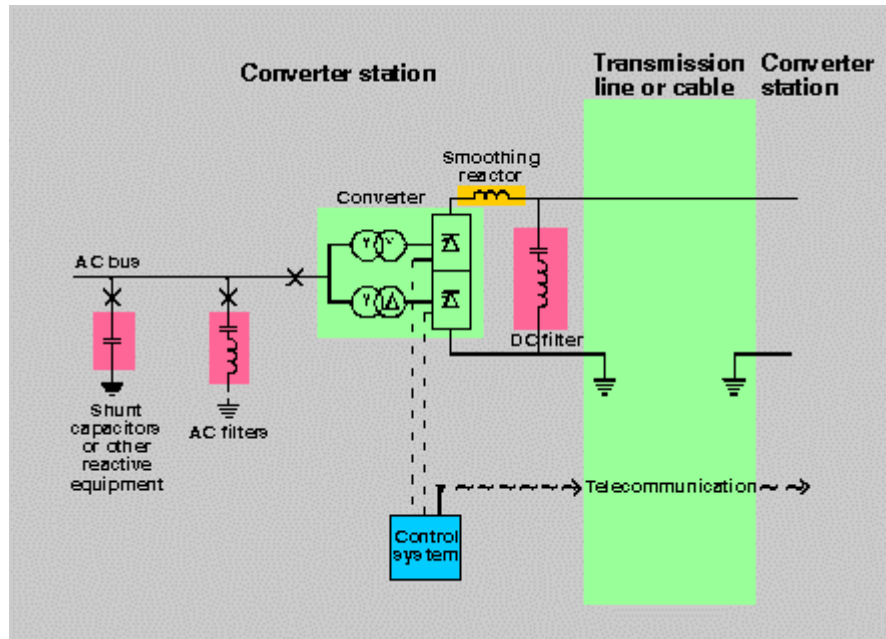


Figure 1.1 A 12 pulse converter bridge

1.2.1 HVDC Classic

The conventional HVDC transmission is called HVDC Classic and is based on a current source converter (CSC), which is a line-commutating converter. The valves in the converter are made out of several thyristors connected in series. The valves are then connected in so called Graetz bridge modules, as shown in figure 1.2.

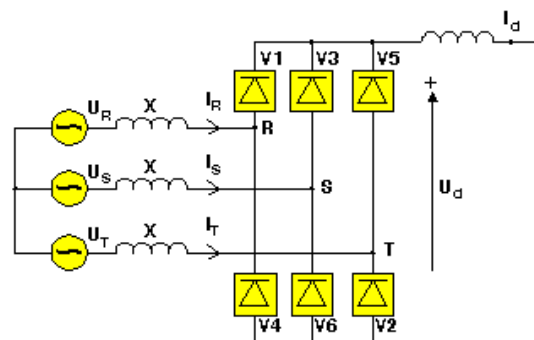


Figure 1.2 The Graetz bridge

A 12 pulse converter bridge can then be built by connecting two Graetz bridges in series. The bridges are then connected separately to the AC system by means of converter transformers, one of Y-Y winding structure and another Y-Δ winding structure, as shown previously in Figure 1.1.

Regarding operation and control of an HVDC link, two basic methods of the gate pulse generation for the valves in the converter are discussed below.

- Individual phase control (IPC).

It was used in early HVDC projects. The main feature of this scheme is that the firing pulse generation for each phase (or valve) is independent of each other and the firing pulses are rigidly synchronised with the commutation voltages. The major drawback of IPC scheme is the aggravation of harmonic stability problem, characterised by magnification of noncharacteristic harmonics in steady state.

- Equidistant pulse control (EPC).

In this scheme, the firing pulses are generated in steady state at equal intervals of $1/pf$, where p is number of pulses and f is the fundamental frequency. There are three variations of the EPC scheme

Pulse frequency control (PFC)

Pulse period control

Pulse phase control (PPC)

All those three schemes are described in detail in [3]. Although EPC scheme has replaced IPC scheme in modern HVDC projects, it has certain limitations. The first drawback is that under unbalanced voltage conditions, EPC results in less DC voltage compared to IPC. EPC scheme also results in higher negative damping contribution to torsional oscillations as shown in Figure 1.3 [3], and it gives more impact when HVDC is the major transmission link from a thermal station.

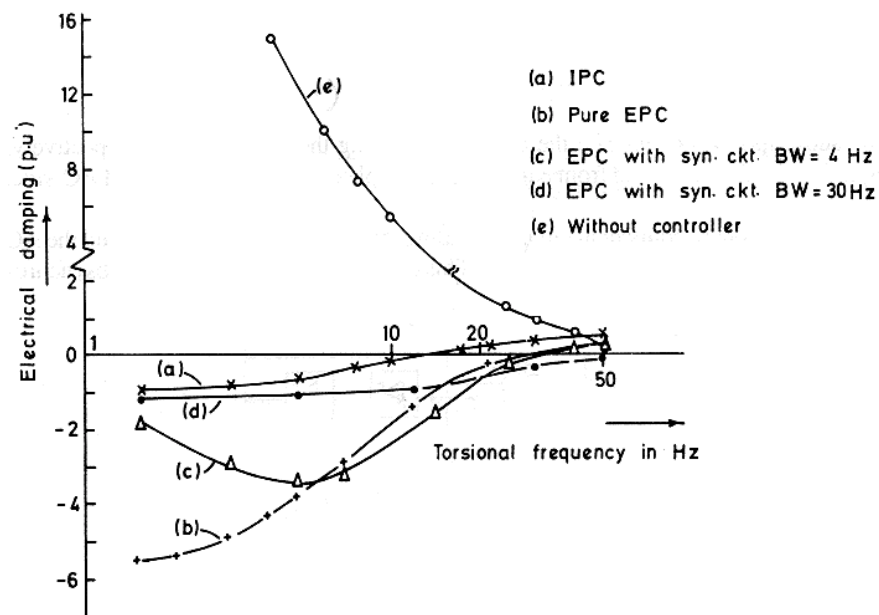


Figure 1.3 Electrical damping for IPC/EPC (with and without synchronising circuit)

1.2.2 HVDC Light

HVDC Light is the latest technology to transfer power by means of HVDC. The first project using Light technology with insulated gate bipolar transistors (IGBT) was a 10 km long test transmission link between Hellsjön and Grängesberg, located in the central part of Sweden. The project transmitted 3 MW and was commissioned in March 1997. HVDC Light is based on a voltage source converter (VSC), which is a self-commutating converter. The valves are made out of turn-off devices using modules of IGBTs with antiparallel-connected diodes. The method uses pulse width modulation (PWM) with a very high switching frequency. The

development of HVDC Light technology within ABB is being made in different stages, which are called generations. The first generation using forced commutation was called generation A. The schematic of it is shown in Figure 1.4.

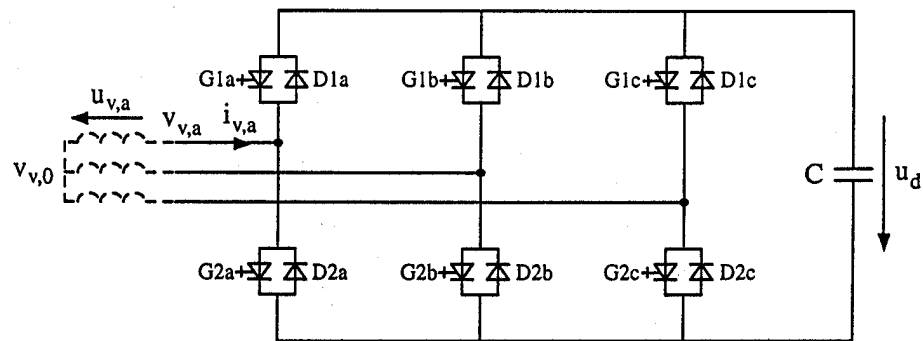


Figure 1.4 The two level converter bridge

Forced commutation gives Light technology the following advantages [7]:

- 1) The converter works independently of any AC source, which makes it less sensitive for disturbances in the AC network and AC faults do not drastically affect the DC side,
- 2) The reactive power to/from the converter can be controlled continuously and independently of the active power flow,
- 3) The converter can be connected to a weak or dead AC network,
- 4) The reverse of power flow is done without reversing the DC voltage. This is an advantage in multiterminal schemes and in cable transmissions.

With the new Light technology projects with a lower level of megawatts can still be profitable. In addition, several other new advantages will open a wide field for new applications. Some of the new applications that now are possible for HVDC are listed below (detailed presentation is available on the Internet [9]):

- Wind power;
- Feed small local loads, e.g. islands;
- Oil platforms;
- Small scale generation;
- Multiterminal DC grid;
- City center infeed;

The new generation B is presented in chapter 4.

2 Problem description and investigation approach

2.1 Problem description

The purpose and major portion of this diploma work was to study the nature of possible HVDC Light subsynchronous torque interaction with nearby generators, and to develop a thorough understanding of the phenomenon. After that the development of RTAS for the Light_B concept had to be done for SSTI investigation and other studies, such as verification of control action and computer based simulations.

The extension of the present work scope means that the operation of VSC converter has to be investigated and possible ways of SSTI have to be studied. This is needed because of SSTI that can result in severe damage of the generator shaft. Shaft damage can also occur due to fatigue when the peak torque exceeds a limit over a certain time period. Risk for SSTI is investigated today using methods developed for classic HVDC, but the mechanism of interaction for HVDC Light has not yet been studied. Following are the approaches of investigation.

2.2 SSTI study

A power system and a generator may interact with subsynchronous effects in several ways. Subsynchronous torque interaction phenomenon is one of them. Therefore, in the first stage of the development work the way of performing SSTI studies for conventional HVDC is reviewed, to find out pointers of how it should be done for Light technology and which are the main points of consideration. It pursues the nature of such problem for suggesting the ways to investigate SSTI in HVDC Light systems.

2.3 Details of HVDC Light_B

The second stage of the development work was to bring up as much as possible information about HVDC Light_B. Since this is quite new technology, the entire material for detailed studies is not available and therefore a large extent of time was used for the literature and information gathering. Attention was paid to the main principles of operation and control strategy.

2.4 SSTI in HVDC Light_B

In this main part of work the nature of possible subsynchronous torque interaction in connection with HVDC Light_B is studied. The attention is concentrated on the behavior of converter related to generator natural swinging. That means the electrical damping of the subsynchronous frequencies is investigated and the interaction mechanism is explained.

2.5 RTAS set-up

The final part of the work was to structure and prepare the set-up of an analogue simulator for future verification of the conclusions of this work and other types of studies. A challenging item was to define the interface between the new valve model and the control system.

3 SSTI related to HVDC Classic

The first experience of HVDC interaction with turbine-generator torsional vibration occurred at Square Butte Electric Coop Project in North Dakota in 1977, where tests had been planned to determine the impact of a special power modulation control applied to the HVDC terminal on turbine-generator torsional vibrations at the adjacent unit. The test showed that the relatively high gain power modulation control did indeed destabilise the first torsional mode of vibration at 11,5 Hz. Field modifications were made initially, which allowed operation under limited conditions. These were immediately followed by an analysis of the interaction, which led to control system modifications [1] that allowed stable operation under all but extreme system contingencies. Thus, there are some applications for which supplementary damping controls for HVDC converters are essential to insure a net positive damping contribution to torsional modes of vibration for all turbine-generator units in the vicinity of the HVDC system.

3.1 Interaction mechanisms

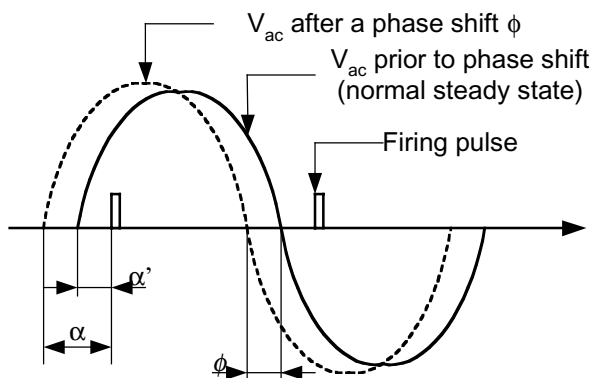
The interaction between turbine-generator shaft vibrations and HVDC systems consists of four basic transfer functions:

- 1) From generator shaft speed to DC current independent of HVDC control action
- 2) From the dc current regulator output to generator shaft torque independent of shaft speed
- 3) The DC current regulator and HVDC system
- 4) From generator shaft speed to torque independent of HVDC control action

There are three primary mechanisms involved in the first and last transfer functions, i.e., from generator shaft speed to HVDC current and generator electrical torque. The first one involves the change in AC voltage magnitude due to a change in generator shaft speed. This arises from the speed voltage effect of an electrical machine with constant flux linkages. As shown in [1], this effect has primary influence over the interaction at frequencies above 15 to 20 Hz for typical systems with equidistant firing.

The second mechanism involves the change in AC voltage magnitude at the rectifier bus due to a change in generator angle based upon the conventional steady-state AC phasor network solution. This effect is only important at low frequencies and with a moderate parallel AC transmission system. For the case of radial operation, this mechanism has virtually no impact on the torsional interaction.

The third mechanism arises with equidistant firing control and is caused by a change in firing angle due to a shift in the voltage phase of the AC network following a change in generator angle, as illustrated in Figure 3.1. This mechanism has primary influence over the interaction below 15 to 20 Hz.



α - actual firing angle following shift in V_{ac} ;

α - pre-shift steady state firing angle;

$\alpha = \alpha' + \phi$;

Figure 3.1 Effect of AC voltage phase shift on firing angle with equidistant firing scheme

The following simplified analysis provides a basis for understanding the influence of these major interaction mechanisms. Consider the case of a turbine-generator having an HVDC system as its only load. The commutating voltage magnitude and phase closely follow generator internal voltage and angle, i.e.,

$$U_{L\Delta} = U_{L0} + \Delta U_L \cong U_{L0} (1 + \Delta\Psi_G + \Delta\varpi_G) \quad (3.1)$$

$$\delta_{c\Delta} = \delta_{c0} + \Delta\delta_c \cong \delta_{c0} + \Delta\delta_G \quad (3.2)$$

where U_L = commutating bus voltage magnitude;

δ_c = commutating bus voltage phase angle;

Ψ_G = per unit internal generator flux;

ϖ_G = per unit generator shaft speed;

δ_G = generator angle.

Subscript 0 implies initial value. Δ implies change.

Neglecting the changes in flux linkages and noting that generator angle is the integral of generator speed,

$$\Delta U_L \cong U_{L0} \Delta\varpi_G \quad (3.3)$$

$$\Delta\delta_c \cong \frac{\omega_{base}}{s} \Delta\varpi_G \quad (3.4)$$

where ω_{base} is angular speed of AC system.

To relate these changes to DC quantities,

$$U_v = K_1 U_L \cos \alpha \quad (3.5)$$

$$\Delta U_v = K_1 (\Delta U_L \cos \alpha_0 - U_{L0} \sin \alpha_0 \Delta \alpha) \quad (3.6)$$

where U_v = voltage behind commutating impedance;

K_1 = constant including bridge characteristics and transformer turns-ratio;

α = actual firing angle.

With equidistant firing system, firing angle is directly related to the AC phase angle, and a separate synchroniser and/or the DC regulator is required to maintain synchronism. This can be expressed mathematically as

$$\Delta \alpha = \Delta \alpha_R + K_p(s) \Delta \delta_c \quad (3.7)$$

where α_R = firing angle command of DC regulator;

$K_p(s) = 0$ for equivalent firing;

= 1 for equidistant firing;

= $[1 - \text{SYNC}(s)]$ for equidistant with a synchronising circuit whose transfer function is $\text{SYNC}(s)$.

Combining equations 3.3 to 3.7 to eliminate commutating bus quantities gives the relationship from generator speed and regulator output to DC voltage:

$$\Delta U_v = K_1 U_{L0} \left[\cos \alpha_0 - K_p(s) \left(\frac{\omega_{base}}{s} \right) \sin \alpha_0 \right] \Delta \varpi_G - K_1 U_{L0} \sin \alpha_0 \Delta \alpha_R \quad (3.8)$$

Quantities of particular interest are DC current and generator electrical torque. DC current is directly related to DC voltage difference. Assuming the inverter to be relatively stiff, only rectifier voltage need be considered; hence,

$$\Delta I_{DC} = Y_{DC}(s) \Delta U_v \quad (3.9)$$

where $Y_{DC}(s)$ is the admittance of the DC system.

DC power is

$$\Delta P_{DC} = \Delta(U_v I_{DC}) = \Delta U_v I_{DC0} + U_{v0} \Delta I_{DC} = [I_{DC0} + U_{v0} Y_{DC}(s)] \Delta U_v \quad (3.10)$$

Generator torque is

$$\Delta T_e = \Delta \frac{P_{DC}}{\varpi_G} = \Delta P_{DC} - P_{DC0} \Delta \varpi_G = [I_{DC0} + U_{v0} Y_{DC}(s)] \Delta U_v - P_{DC0} \Delta \varpi_G \quad (3.11)$$

Changes in generator torque and DC current are directly related to changes in DC voltage, as shown by Equations 3.9 to 3.11. Hence, the relationships to generator speed and DC firing angle defined by Equation 3.8 also apply directly to DC current and generator torque.

For purely equidistant systems, it can be seen from Equation 3.8 that the mechanism of a firing angle change due to a phase shift in the AC voltage introduces an integral characteristic in the transfer functions from shaft speed to DC quantities, proportional to the sine of the firing angle. The frequency at which the integral term equals the proportional term (which is due to the speed voltage effect) is equal to the product of the system base frequency and the tangent of the

firing angle. In [1] is noticed, that the synchronising circuit does not wash out the interaction to zero at low shaft modulation frequencies, but only prevents the gain from increasing further at lower frequencies.

In other words if the generator speed increases at the rectifiers side due to inherent subsynchronous shaft oscillations, and firing pulse time stays the same, then the firing angle α becomes bigger, as shown in Figure 3.1. It leads to lower DC voltage value resulting in decreased transmitted DC power. So the response has negative characteristic and does not damp the oscillations. The same mechanism but in opposite direction is involved when the generator speed decreases, therefore the HVDC link in both cases contributes with negative subsynchronous oscillations damping.

Using the same approach as for the rectifier, it can be shown that the inverter has positive subsynchronous oscillations damping.

The second part of the interaction discussed at the beginning of this subsection involves the impact of the controller output, α_R on generator torque. The essential part of this transfer function appears in the second part of Equation 3.8, indicating that the gain is proportional to the sine of the steady-state firing angle. This is a well-known relationship, and in some HVDC controllers a special network is included to linearize the gain over a nominal firing-angle operating range.

3.2 Screening study

The interaction between an HVDC converter and a machine can be assessed by means of the unit interaction factor (UIF). If it is higher than 0,1, then there will be a risk of SSTI [1]. These assessment calculations are always made within an HVDC project in a so called screening study . If this study shows that there is no risk of adverse interaction, no further SSTI detailed study will be made.

The UIF is calculated as follows

$$UIF_i = \frac{MW_{HVDC}}{MVA_i} \left(1 - \frac{SC_i}{SC_{tot}} \right)^2 \quad (3.12)$$

UIF_i	: Unit interaction factor of the i:th unit
MW_{HVDC}	: MW rating of the HVDC system
MVA_i	: MVA rating of the i:th machine
SC_i	: Short circuit capacity at the commutating bus excluding the i:th unit
SC_{tot}	: Short circuit capacity at the commutating bus including the i:th unit

3.3 Detailed study

In the detailed SSTI study the investigation is concentrated on determining the electrical damping for the actual generator unit. This study is usually performed in EMTDC and is called one mass model study. For determining the damping, a disturbance signal is injected into the system. The signal is scanned from 2 to 40 Hz and is added to the speed order of the machine while the electrical damping of the injected signal is continuously calculated.

The electrical damping is calculated using the formula below.

$$D_e = \text{Re} \left(\frac{\Delta T_e}{\Delta \omega_e} \right) \quad (3.13)$$

where

D_e is the electrical damping

Re means the real part of value

ΔT_e is the change in electrical torque

$\Delta \omega_e$ is the change in electrical speed

3.4 SSDC

If there is a negative or very low damping of any critical frequency, a subsynchronous damping controller (SSDC) is required. A damping controller is developed and integrated in the converter control system. It increases the damping at the critical frequencies by adding a small signal to the rectifiers signal, which determines the firing instant. For classical applications, the magnitude of this signal is typically a fraction of a degree. The SSDC has to be adapted to each new project.

The two level bridge shown previously in Figure 1.3 is the most simple circuit configuration, that can be used for building up a three phase forced commutated VSC bridge. The three level or Neutral Point Clamped (NPC) converter bridge is a very interesting alternative in high power applications due to the fact that the phase potentials can be modulated between three levels instead of two. The advantage of such configuration is reduced harmonic content in the bridge voltage for a given switching [2]. It also allows using simple transformer connection and the amplitude of the fundamental (50 or 60 Hz) AC output voltage can be varied from the controller directly without changing the DC voltage or transformer ratio. The principals of operation for the three level bridge are also relatively simple. Each phase can be connected to the positive DC terminal, the midpoint or the negative DC terminal. Compared to the two level bridge, the three level bridge requires six extra diodes connected to the midpoint on the DC side.

An equivalent circuit of the VSC connected to a three phase AC network is shown in Figure 4.1. The converter bridge can be connected to the AC network via a transformer, but it is also possible to do that connection via phase inductors [2]. The converter can be represented as a variable AC voltage source where the amplitude, the phase and the frequency can be controlled independently of each other. It means that the VSC bridge can be seen as a very fast synchronous generator with the instantaneous phase voltage $u_{v,x}$, as shown in expression 4.1. The coupling function k_x describes how the bridge phase voltage $u_{v,x}$ depends on the DC voltage u_d . The instantaneous value of k_x is determined by the control of the valves.

$$u_{v,x}(t) = k_x(t)u_d(t) \quad (4.1)$$

where $x = a, b$ or c .

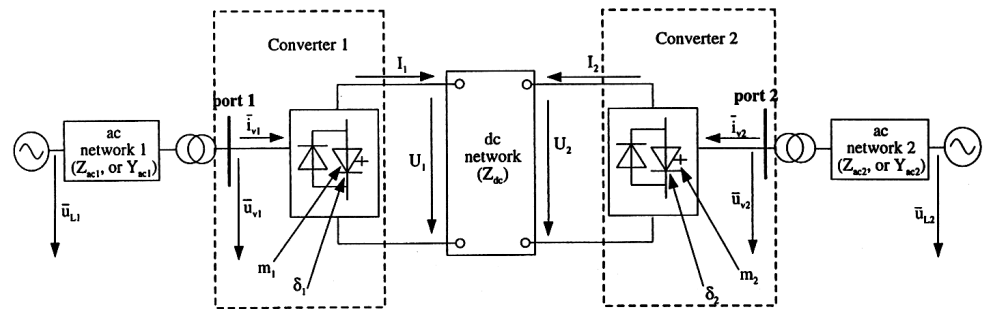


Figure 4.1 Voltage source converter connected to an AC network

In steady state, the fundamental frequency components of the phase voltages and the phase currents can be represented by phasors according to Fig. 4.2. Symmetrical three phase voltages and currents are assumed, i.e. only positive sequence quantities exist. Phasor representation is useful when the active and reactive power flows on the AC side are analysed. The voltage and currents on the DC side determine the power flow on the DC side. Subscript (1) implies positive sequence.

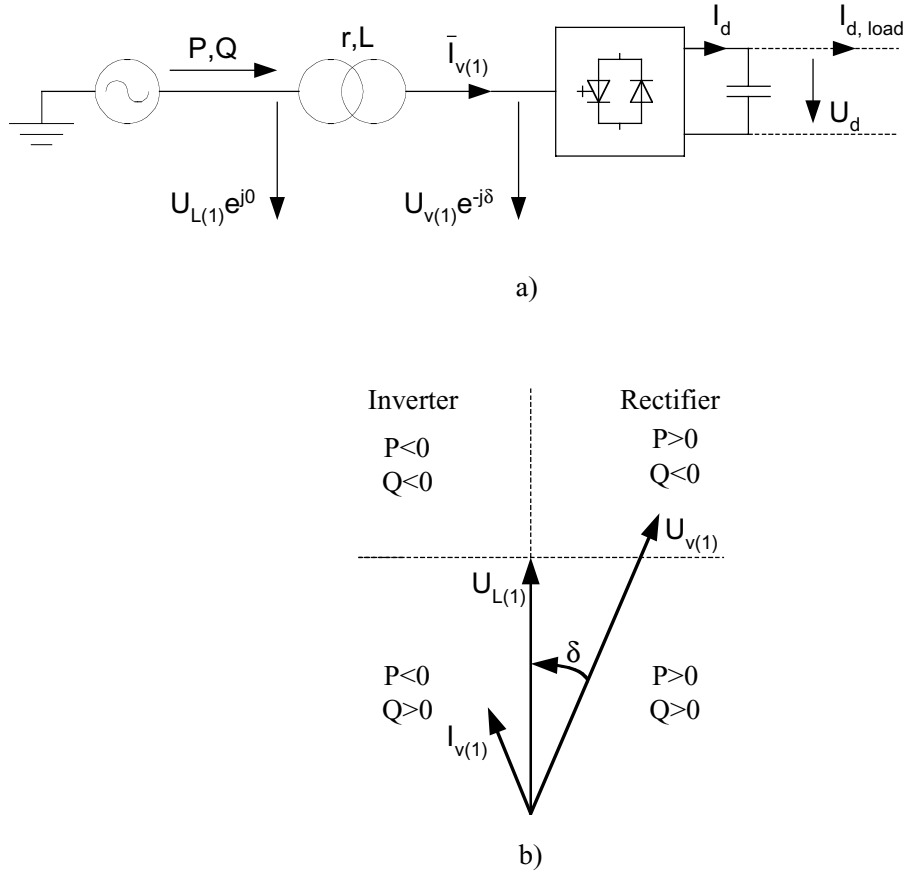


Figure 4.2 a) VSC connected to an AC network (phasor representation),
b) Phasor diagram (fundamental) and direction of power flows. The location of the U_{v1} phasor determines the operation mode (rectifier or inverter)

With phasor representation, the fundamental AC bridge voltage is given by the fundamental frequency component of the coupling function and the DC voltage, according to Eq. 4.2.

$$\bar{U}_{v(1)} = \bar{K}_{(1)} U_d \quad (4.2)$$

The fundamental apparent power in the connection point of the converter is defined as

$$\bar{S} = P + jQ = 3 \cdot \bar{U}_{L(1)} \bar{I}_{v(1)}^* \quad (4.3)$$

In high power applications the resistance r (transformer or inductor resistance) is small and can be neglected. The active power and the reactive power drawn from the AC network by the converter then become

$$P = 3 \cdot \frac{U_{L(1)} \cdot U_{v(1)}}{\omega L} \cdot \sin \delta \quad (4.4)$$

$$Q = 3 \cdot \frac{U_{L(1)} \cdot (U_{L(1)} - U_{v(1)} \cos \delta)}{\omega L} \quad (4.5)$$

The angle δ is the phase shift between the line side AC network voltage $U_{L(1)}$ and the fundamental bridge side voltage $U_{v(1)}$ according to figure 4.2. A positive phase shift means that the line voltage is leading the bridge voltage and that active power flows into the converter. The phasor diagram in Fig. 4.2b indicates how the signs of the active and reactive powers depend on the phase and the amplitude of the converter bridge voltage if the line voltage phasor is assumed constant.

Equation 4.4 gives that the active power consumed or generated by the VSC mainly depends on the phase shift angle δ . From Equation 4.2 it can be realised that the phase of the fundamental bridge voltage is determined by the phase of the fundamental frequency coupling function. It is then possible to express the phase shift according to Equation 4.6.

$$\delta = \arg(\overline{U}_{L(1)}) - \arg(\overline{U}_{v(1)}) = \arg(\overline{U}_{L(1)}) - \arg(\overline{K}_{(1)}) \quad (4.6)$$

Thus the active power can be controlled relatively fast by changing the phase of the fundamental coupling function.

The active power transmitted from the DC side in steady state is

$$P_d = U_d \cdot I_{d,load} \quad (4.7)$$

The direction of the power is given by the sign of the direct current $I_{d,load}$ since the polarity of the DC side voltage U_d remains unchanged for a VSC.

The active power flow on the AC side must equal the active power transmitted from the DC side in steady state (losses disregarded). This can be fulfilled in an HVDC connection if one of the two converters controls the active power transmitted at the same time as the other converter controls the DC voltage. With a single VSC connected as an SVC ($I_{d,load} = 0$) and no losses assumed, there can not be any active power flow in steady state. In this case, the active power control is only used to control the DC voltage.

The reactive power consumed or generated by the VSC is mainly determined from the difference in amplitude between the line voltage and the bridge voltage according to Eq. 4.5. The amplitude of the fundamental bridge voltage is given by the amplitudes of the DC voltage and the fundamental coupling function, i.e.

$$U_{v(1)} = K_{(1)} \cdot U_d \quad (4.8)$$

The reactive power can be controlled in two ways, either by changing the DC voltage or the amplitude of the fundamental coupling function. If the reactive power is controlled with the DC voltage, the speed of response is determined by the size of the DC side capacitor. This type of control becomes rather slow. However, by introducing Pulse Width Modulation (PWM), the coupling function can be changed and a relatively fast control of the reactive power can be obtained. Also in order to control the reactive power independently of the active power in an HVDC, at least one of the converters has to be able to vary the amplitude of the coupling function.

With a pulse width modulated bridge voltage it is also possible to implement an inner current loop control and thereby further increase the speed of the response in the active and reactive power loops.

4.1 The three level converter bridge

The three level bridge shown in fig. 4.3 is a very interesting alternative to the two level bridge in high power applications because the phase potentials can be modulated between three levels instead of two.

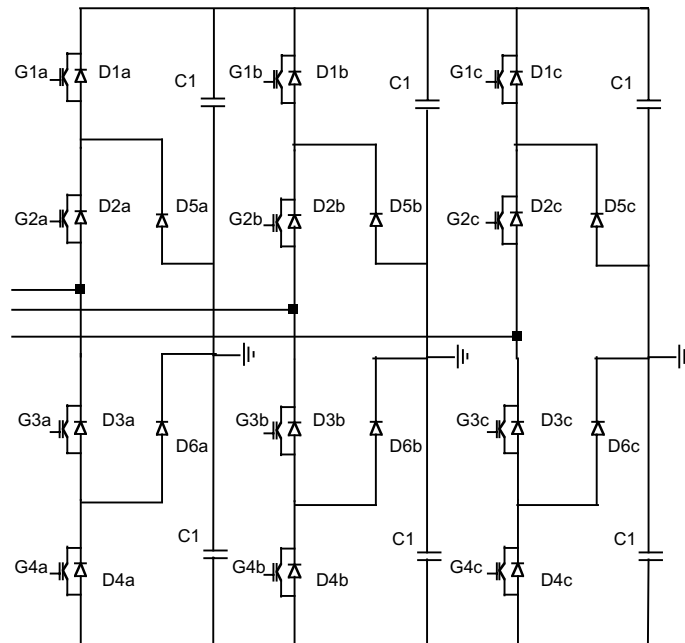


Figure 4.3 Three level Voltage Source Converter configuration

The principles of operation for the three level bridge are also quite simple. Each phase can be connected to the positive DC terminal (G1x/G2x on, G3x/G4x off), the midpoint on the DC side (G2x/G3x on, G1x/G4x off) or the negative DC terminal (G3x/G4x on, G1x/G2x off). There is only one switching required when the connection point changes from the positive, or negative, DC terminal to the midpoint on the DC side.

Compared to the two level bridge, the three level bridge requires six extra diodes connected to the midpoint on the DC side, as indicated in fig. 4.3. The total number of switching devices used in valves will, however, not increase on condition that series connection of switching devices is required in order to build up each valve. This is because the blocking voltage of each valve is $u_d/2$, which is half the blocking voltage of each valve in a six pulse bridge. Therefore, the number of switching devices required to build up each valve is half as many for the three level bridge than for the two level bridge.

It can also be shown that the total switching losses within the two level and three level converter bridges, for operation with the same switching frequency per valve, are comparable if it is assumed that the switching losses are proportional to the blocking voltage of each valve. The total losses (switching and conduction losses) for the two level and three level bridges respectively has, however, to be further analysed before any final conclusions can be drawn.

The three level bridge configuration implies that the DC side capacitor is split up in two parts, which can cause DC voltage unbalance. It is possible to keep the DC side voltages balanced (i.e. $u_{d1}=u_{d2}$) if a DC voltage balance control is added to the converter control as shown in [2]. The balanced control proposed is based on that carrier based PWM is used, i.e. a relatively high switching frequency. In order to keep the DC side balanced at fundamental switching frequency operation, a temporary increase of the switching frequency is required at DC side unbalance.

A simplified switch representation for the analysis can be applied for the three level bridge. The three level bridge shown in fig. 4.3 can be simplified according to fig. 4.4, where each leg is represented by a three level switch.

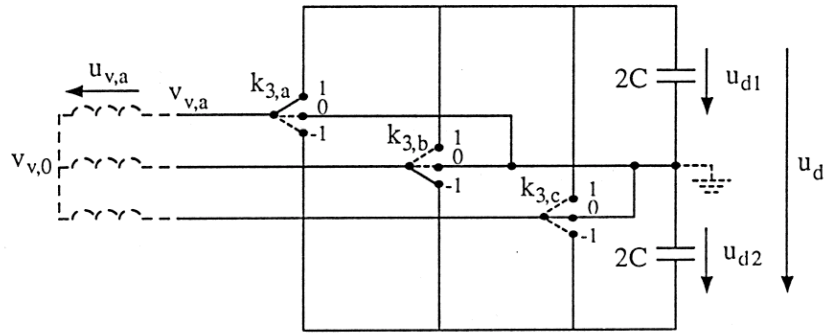


Figure 4.4 The three level bridge, switch representation

The relationship between the coupling function $k_{3,x}$ and the states of the valves in phase x is shown in Table 4.1.

Table 4.1

	G1x	G2x	G3x	G4x
$k_{3,x}=1$ ($k_{3u,x}=1, k_{3l,x}=0$)	on	on	off	off
$k_{3,x}=0$ ($k_{3u,x}=0, k_{3l,x}=0$)	off	on	on	off
$k_{3,x}=1$ ($k_{3u,x}=0, k_{3l,x}=1$)	off	off	on	on
Forbidden state	on	off	off	on

It is possible to express the phase potentials referred to the midpoint on the DC side according to eq. 4.9.

$$v_{v,x} = k_{3u,x} \cdot u_{d1} - k_{3l,x} \cdot u_{d2} \quad (4.9)$$

Assuming that the bridge is connected to a transformer without any connection to earth, the phase voltage $u_{v,x}$ becomes equal to the zero-sequence-free part of the phase potential $v_{v,x}$, i.e.

$$u_{v,x} = v_{v,x} - v_{v,0} \quad (4.10)$$

$v_{v,0}$ is the potential of the transformer virtual neutral point referred to the midpoint on the DC side and can be calculated according to eq. 4.11.

$$v_{v,0} = \frac{v_{v,a} + v_{v,b} + v_{v,c}}{3} \quad (4.11)$$

The output voltages in phase a of a three level converter bridge operating with fundamental switching frequency is shown in fig. 4.5. Here, balanced operation is assumed which means that $u_{d1}=u_{d2}=u_d/2$. It is also assumed that the phase voltages (and the phase potentials) are symmetrical, i.e. equal in waveform but phase displaced $2\pi/3$ rad from each other.

The peak values of the fundamental and harmonics in the phase voltage are found by applying Fourier analysis on the phase voltage shown in fig. 4.5b [2].

$$u_{v(n)} = \frac{2}{n \cdot \pi} \cdot u_d \cdot \cos(n \cdot \alpha_1) \quad (4.12)$$

where $n = 1, 5, 7, 11, 13$

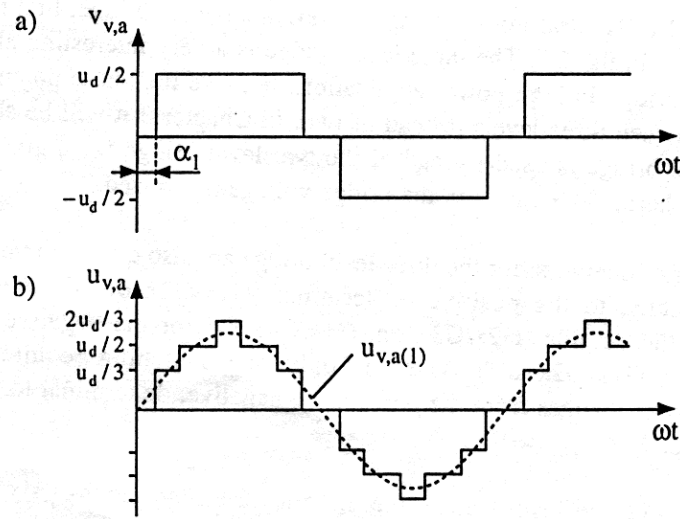


Figure 4.5 Output voltages of a three level bridge operating with fundamental frequency ($u_{d1}=u_{d2}=u_d/2$, $\alpha_1=0.31$ rad (18°)).
a) Phase potential referred to a virtual midpoint on the DC side.
b) Phase voltage on the valve side of a transformer.

From eq. 4.12 it can directly be seen that it is possible to vary the amplitude of the fundamental bridge voltage with the switching angle α_1 and thereby also the ratio between the fundamental bridge voltage and the DC voltage. With the three level bridge, unlike the two level bridge, a pulse width modulated bridge voltage is obtained even for fundamental frequency switching and the reactive power can be controlled rapidly.

The output voltage of the three level bridge can also be described with space vectors [2]. The possible bridge AC voltage vectors are shown in fig. 4.6. There are 27 combinations of $k_{3,a}$, $k_{3,b}$ and $k_{3,c}$ and the bridge voltage vector can reach 19 different points in the $\alpha\beta$ -plane. The zero voltage vector can be reached by three combinations. The active states correspond to voltage vectors with three different amplitudes and twelve different directions in the complex plane. The length of the voltage vectors are $2/3u_d$ (full voltage vectors), $1/3u_d$ (half voltage vectors) and $1/\sqrt{3}u_d$ (intermediate voltage vectors). It should be observed that the six half voltage vectors could be obtained in two ways.

Due to the limited power rating of the converters, the independent control of the active and reactive power within a station may be limited to a certain operation range.

The complete control system of a VSC consists of the Master Control and the Basic control [2]. The Master control consists of DC voltage reference regulation, Active power reference regulation, DC voltage control, DC overvoltage & undervoltage control, AC voltage control, Current order calculation and Current order limiter. In addition to the current references, the control signals for the tap-changer are also generated in the Master control. In order to secure all the different control functions, a Sequence control is also included in the Master Control. The Basic control is composed of Phase locked loop, AC current control and PWM. The output of the Basic Control will be sent to the converter valve control.

5 SSTI in HVDC Light

The mechanism of subsynchronous torque interaction in HVDC Light will be shown using the same approach as for Conventional HVDC for easier understanding. The response of the HVDC Light converter to the variation of frequency due to inherent subsynchronous generator shaft oscillations will be investigated. The configuration shown in Figure 5.1, a voltage source converter connected to the AC bus via reactance ωL , will be used for this purpose.

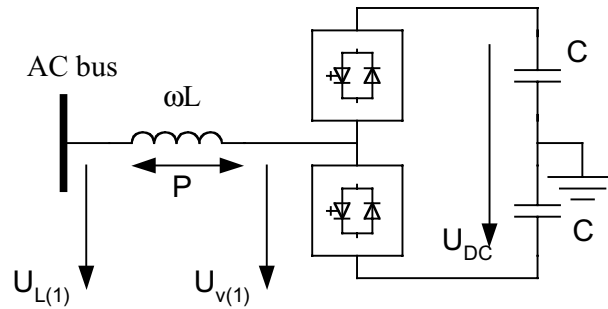


Figure 5.1 VSC connected to AC bus

Remembering, that damping is defined as a real part of the ratio between change of electrical torque and change in electrical speed as shown in the formula below

$$D_e = \text{Re} \left(\frac{\Delta T_e}{\Delta \omega_e} \right) \quad (5.1)$$

and change in electrical torque is defined as

$$\Delta T_e = \Delta \frac{P_{DC}}{\omega_G} \quad (5.2)$$

From the formulas written above it is obvious that the item, which defines the sign of the damping is the active power. Therefore, the character of converter power response to the frequency deviation will be investigated.

Again, the main equation describing the active power flow in VSC is (5.3).

$$P = 3 \cdot \frac{U_{L(1)} \cdot U_{v(1)}}{\omega L} \cdot \sin \delta \quad (5.3)$$

We assume that converter side voltage stays constant during the frequency change and no control action is taken, then the frequency change will affect the angle between converter side voltage and AC bus voltage.

For rectifier this process is illustrated in vector diagram in Figure 5.2

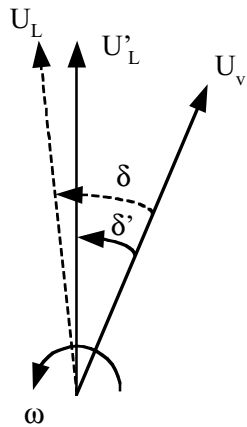
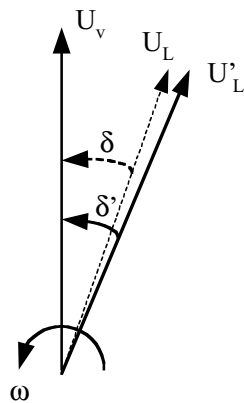


Figure 5.2 shows the case when the frequency increases, the angle δ also increases and becomes δ . The active power flow to the converter will become higher, since it is a sinusoidal function of the angle δ , as shown in Equation 5.3. That means that the sign of the damping would be positive and the subsynchronous oscillations will be damped.

Following the same sequence it can be shown, that during the frequency decrease the angle δ would decrease, which will result in an active power flow reduction.

Figure 5.2 Rectifier voltage vector diagram

For the inverter operation active power flow has direction out of converter and vector diagram for voltages will look like in Figure 5.3



Now the mechanism of interaction is still the same, but the active power flow has direction from the VSC. If the frequency at the AC bus increases, the angle between voltages decreases and so does the active power. It would look like inverter has negative damping, but it should be noted that in this case the active power flow is negative from generator point of view. Conclusion is that converter operating as an inverter also contributes with subsynchronous oscillation damping.

The same conclusion can be made for negative frequency deviation, when the angle δ increases and so does the active power.

Figure 5.3 Inverter voltage vector diagram

6 Converter control impact on SSTI in HVDC Light

Effects of converter control on electrical damping are quite difficult to investigate using theoretical approach. That is because the control system for HVDC Light is very complex and sophisticated.

First steps in the development of a SSTI study methodology for HVDC Light with the controls included were made by ABB using the electromagnetic transient simulation software tool EMTDC. The targets and results are presented in [4] and show that HVDC Light converters contribute with higher subsynchronous oscillation damping than Conventional HVDC. The same conclusion is drawn in [5]. The results indicate that in a network configuration characterised by UIF (Unit Interaction Factor) of 0.2 there could be negligibly small interaction between the HVDC Light transmission link and a nearby generator. Figures 6.1 and respectively 6.2 point out that the interaction is much less for the Light concept than for a conventional HVDC transmission. The figures of plots showing different damping characteristics for machine feeding a passive load, active load (conventional HVDC) and active load (HVDC Light) in parallel with infinite bus are presented in Enclosure 1.

In this context, it must also be mentioned that a Japanese investigation of steady-state stability for shaft torsional oscillation in HVDC systems, using self-commutated converters, presents observations and conclusions that design of converter control systems has impact on the SSTI [8]. It is claimed that with some control setting parameters (gains and time constants) the converter will contribute with negative damping and result in unstable shaft torsional oscillations. However, with proper control settings no subsynchronous damping control is needed, what the ABB work seems to be pointing at.

But it is likely to believe, that properly designed control system will not change the characteristic of subsynchronous oscillation damping so significant, that it would become extremely negative. The results of investigation made in ABB confirm that suggestion.

Then, it can be concluded that properly designed controls will have major impact on SSTI.

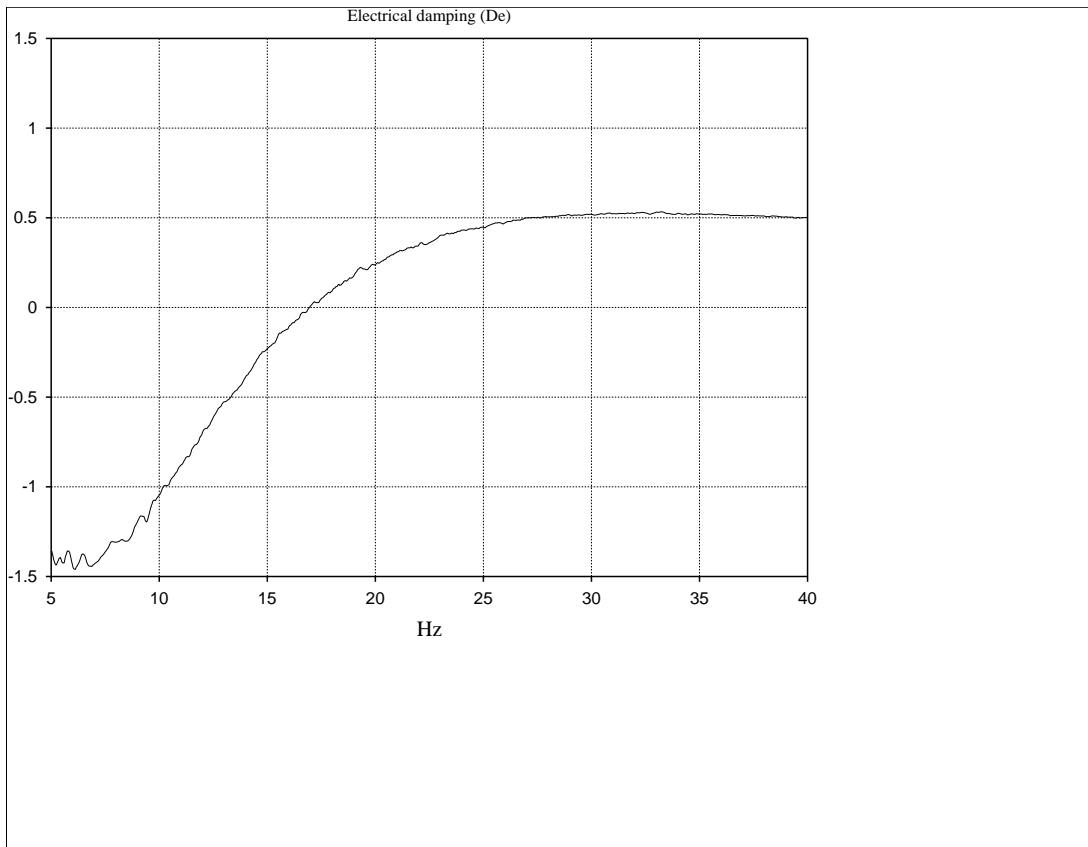


Figure 6.1 Electrical damping curve for the HVDC

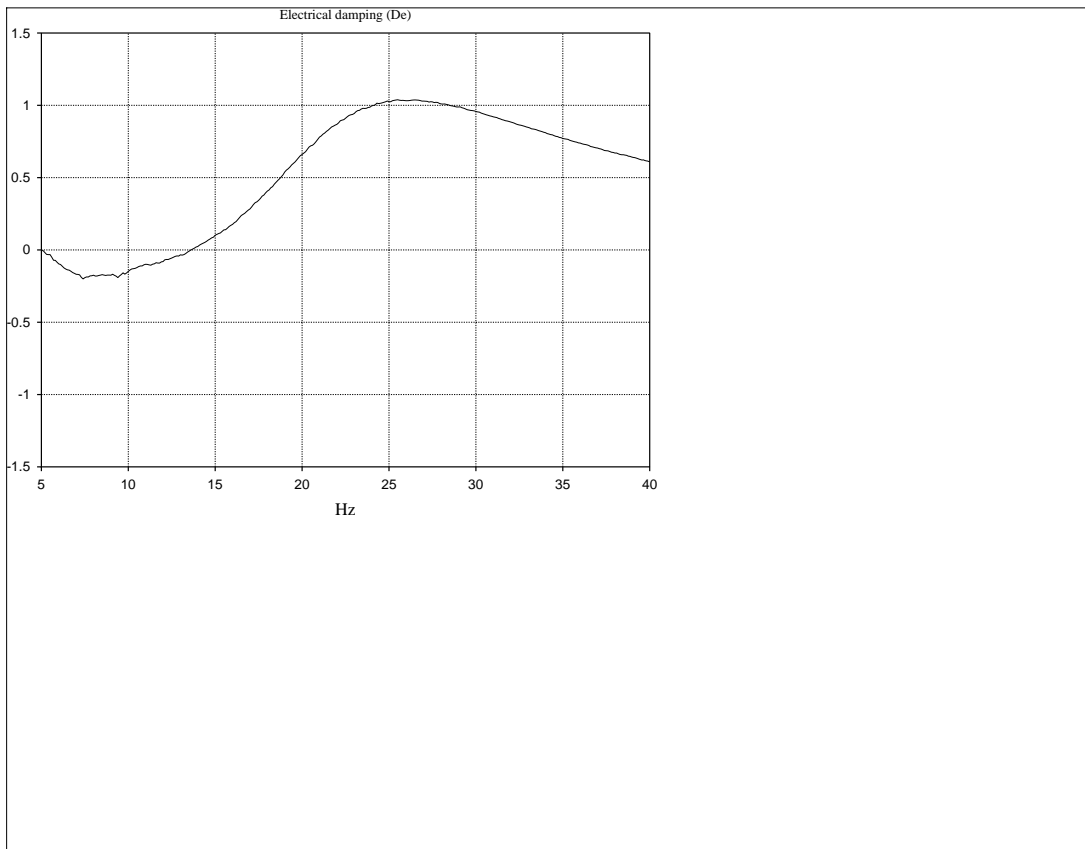


Figure 6.2 Electrical damping curve for the HVDC Light

7 Summary

7.1 Conclusions/suggestions for verification

This report describes the study of subsynchronous torque interaction in HVDC in general and in HVDC Light transmission in particular. Further, the set-up of an RTAS for Light_B verification is described. The conclusions of this diploma work are the following:

- HVDC Light converters connected to the AC network with synchronous generators in vicinity will contribute with positive damping of subsynchronous generator shaft oscillations. This is theoretical conclusion, based on the assumption that no controls take action. It has to be verified with simulation results.
- Effects of control: ABB studies show, that an SSDC is not required if proper settings of control design are made, what is also shown in [8].
- Verification should be made preferably in a real time analogue simulator (RTAS) since in EMTDC the same simulations would take very long time. The reliability of the results obtained in digital simulations will be also verified. General details on RTAS set-up are given in Enclosure 2.

7.2 Recommended continuation

After the work and studies that were done following steps should be taken in further study of SSTI related to HVDC Light and the set-up of the RTAS.

- The set up of the RTAS should be finished connecting the main circuit part to the real controls. The proper operation should be verified for the simulator ability to transmit and control the power.
- The study of SSTI in HVDC Light without and with control action in RTAS should be made to verify the theoretical interaction interpretation.
- Other studies should be performed, such as validation of EMTDC damping, low frequency oscillations, monitoring of flickers generated by HVDC Light, DC ground current, developing of stability measurement tools, etc.
- Further steps in developing SSTI study tools for HVDC Light in EMTDC should be taken and those tools should be verified in RTAS.

8 References

1. Piwko R.J., Larsen E.V., HVDC System Control for Damping of Subsynchronous Oscillations EPRI EL-2708 Research project 1425-1 Final report, October 1982.
2. Lindberg A., PWM and Control of Two and Three Level High Power Voltage Source Converters , KTH, Stockholm, 1995, ISSN-1100-1615.
3. Padiyar K.R., HVDC Transmission Systems , Wiley Eastern Limited, New Delhi, India, ISBN 81-224-0102-3, 1990.
4. ABB Report 1JNL100040-122, First Step in the Development of a SSR Study for HVDC Light , 2000.
5. ABB Report 1JNL100038-979, Preliminary SSR Study for HVDC Light , 2000.
6. ABB Report RTAS for HVDC Light_B , 2001.
7. Lindberg L., Voltage Source Forced Commutation Converters for High Power Transmission Applications , KTH, ISSN 1100-1615, 1990.
8. Steady-state Stability of Shaft Torsional Oscillation in an AC-DC Interconnected System with Self-commutated Converters , Electrical Engineering in Japan, Vol. 128, No. 4, 1999.
9. <http://www.abb.se/powersystems>, (2000), ABB Power Systems AB.

9 Abbreviations

AC	<u>A</u> lternating <u>C</u> urrent
CIGR	<u>C</u> onf rence <u>I</u> nternationale des <u>G</u> rands <u>R</u> seaux <u>E</u> lectriques
CSC	<u>C</u> urrent <u>S</u> ource <u>C</u> onverter
DC	<u>D</u> irect <u>C</u> urrent
EPC	<u>E</u> quidistant <u>P</u> ulse <u>C</u> ontrol
EMTDC	<u>E</u> lectro <u>M</u> agnetic <u>T</u> ransients for <u>D</u> irect <u>C</u> urrent
FST	<u>F</u> actory <u>S</u> ystem <u>T</u> est
HVAC	<u>H</u> igh <u>V</u> oltage <u>A</u> lternating <u>C</u> urrent
HVDC	<u>H</u> igh <u>V</u> oltage <u>D</u> irect <u>C</u> urrent
IGBT	<u>I</u> nsulated <u>G</u> ate <u>B</u> ipolar <u>T</u> ransistor
IPC	<u>I</u> ndividual <u>P</u> hase <u>C</u> ontrol
PLL	<u>P</u> hase- <u>L</u> ocked <u>L</u> oop
PSCAD	<u>P</u> ower <u>S</u> ystem <u>C</u> omputer <u>A</u> ided <u>D</u> esign
PSS	<u>P</u> ower <u>S</u> ystem <u>S</u> tabiliser
PWM	<u>P</u> ulse <u>W</u> idth <u>M</u> odulation
S _{sc}	<u>S</u> hort <u>C</u> ircuit <u>C</u> apacity
SSDC	<u>S</u> ub <u>S</u> ynchronous <u>D</u> amping <u>C</u> ontrol
SSR	<u>S</u> ub <u>S</u> ynchronous <u>R</u> esonance
SSTI	<u>S</u> ub <u>S</u> ynchronous <u>T</u> orque <u>I</u> nteraction
SVC	<u>S</u> tatic <u>V</u> ar <u>C</u> ompensator
UIF	<u>U</u> nit <u>I</u> nteraction <u>F</u> actor
VSC	<u>V</u> oltage <u>S</u> ource <u>C</u> onverter

10 Acknowledgements

I would like to thank everyone at the Department of System Simulations (LST) at ABB Power Systems AB in Ludvika, who have helped me to accomplish this diploma work. Special thanks go to former Manager of this Department Mr. Magnus Lalander, who was kind to respond to my request, and invited me to do my Master Thesis Work in his Department.

I wish to express my gratitude to my supervisors. Special thanks to Mr. Hugo Duch n (ABB Power Systems), for supervising this work, for valuable comments and discussions. Also special thanks to Professor Olof Samuelsson (Lund Institute of Technology), for the supervising and for the careful proof reading. My sincere thanks to my examiner Professor Vaclovas A_ubalis (Kaunas University of Technology) for his constant encouragement and support.

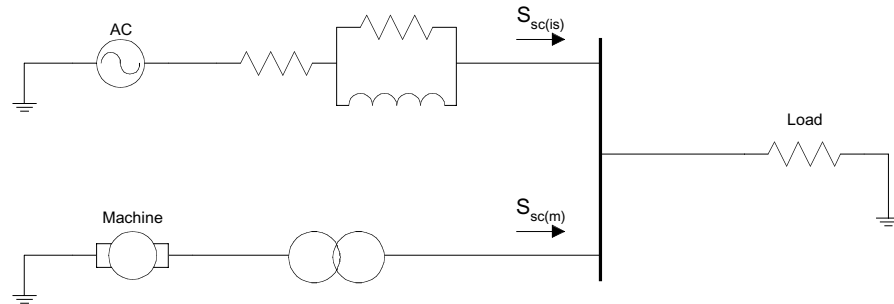
Thanks to my girlfriend Snieguole and all other friends, who did not let me forget my home and sent many teasing messages.

Last but not least, I would like to thank my family for understanding and selfless support.

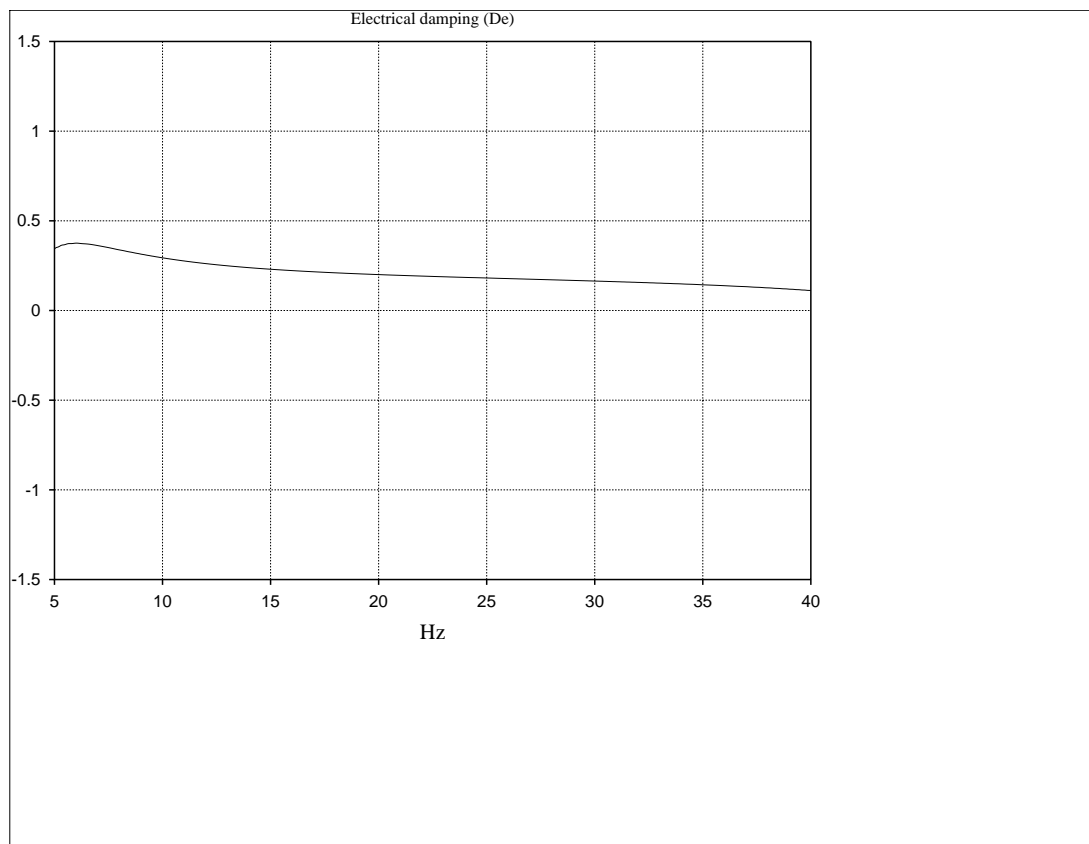
11 Enclosures

11.1 Enclosure 1: Preliminary studies of SSTI in HVDC Light [5]

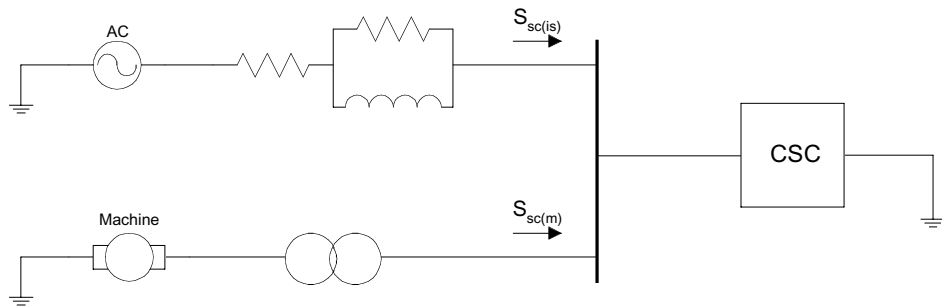
The configuration consists of a machine feeding a passive load of 65 MVA and an infinite bus. This case is a reference case for the comparison.



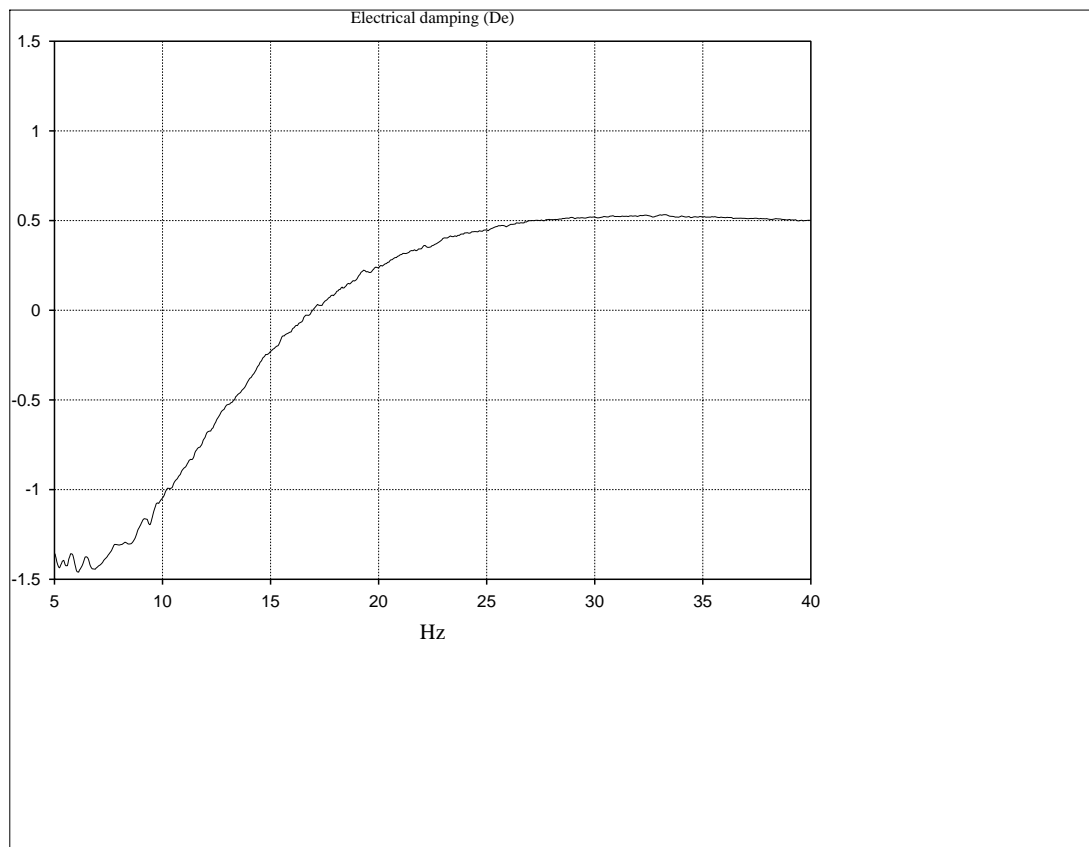
A frequency study was performed on the network configuration above. The disturbance signal injected into the system swept from 40 to 5 Hz. The electrical damping of the network configuration can be seen below.



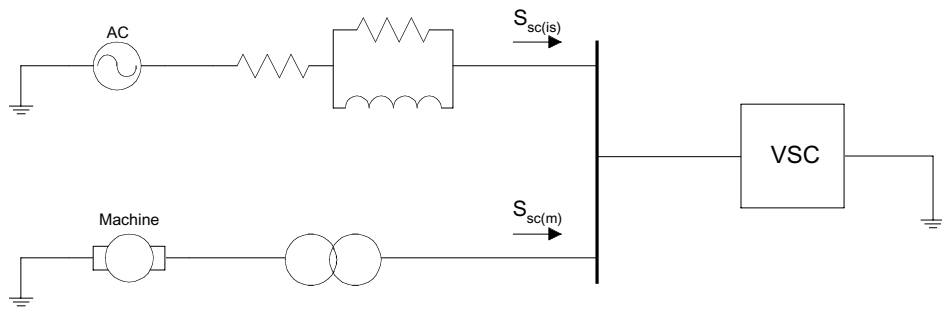
This configuration consists of a machine feeding an active load of 65 MVA and an infinite bus. The active load is a conventional HVDC transmission. The network configuration can be seen below.



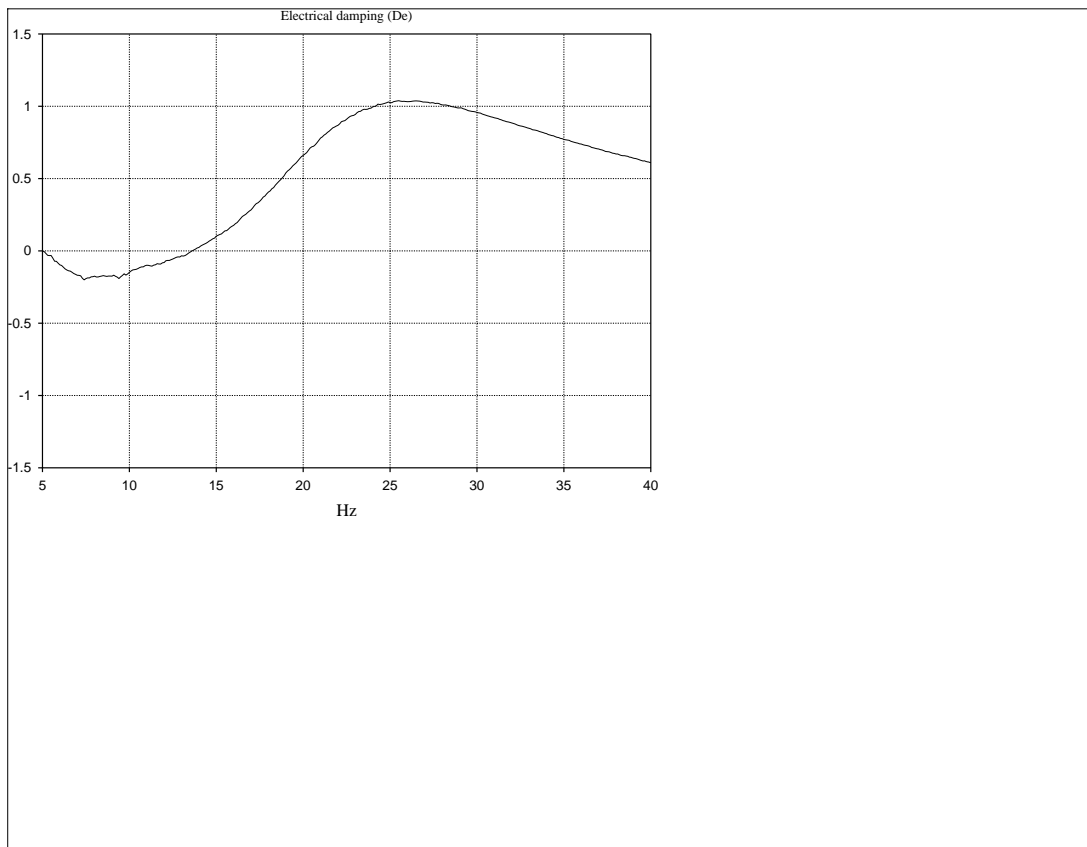
A frequency study was performed. The disturbance signal injected into the system swept from 40 to 5 Hz. The electrical damping of the configuration can be seen in the plot below.



This is the main configuration. It consists of a machine feeding an active load of 65 MVA and an infinite bus. The active load was in this case an HVDC Light transmission link.



A frequency study was performed on the network configuration. The disturbance signal injected into the system swept from 40 to 5 Hz. The resulting plot of the electrical damping curve for this network configuration can be seen below.



11.2 Enclosure 2: RTAS set-up

The set-up of the Real Time Analogues Simulator is a part of the whole simulator development. For the main circuit, shown in section 11.2.6, component models were used from previous HVDC Light_A analogue simulator. The task was to set up the new configuration by modifying existing models and introduce some new components. The whole scope of the work can be seen from the work time schedule in section 11.2.7. The block layout is also available in section 11.2.8.

The first step of set-up work was to become familiar with documentation of previous project in order to define the changes that should be made. Mainly, the modification comprehended introduction of extra reactance in power transformer model, moving of AC filters and PLC filters into another rack because of totally different model configuration and tuning, and connecting of new valve model and new DC cable model to the whole simulator. Power supply question and some other minor changes (additional reactance in infinite bus rack, reactances to represent step up transformers etc.) were also solved.

11.2.1 Digital machine set-up

This task was one of the most complex and time consuming.

The synchronous machines are represented with real-time digital model, developed at ABB Power Systems AB, Ludvika. The basic idea of the digital machine model is to generate a three-phase voltage, depending on its internal parameters and also on the current flowing into the network where the machine is connected.

The setting up for a specific machine is done by means of a PC, in which the pre-processing software as well as the real-time programs is stored in different subdirectories. The PC will only be necessary for setting up the model and loading the program into the machine hardware. After setting up and loading the machine the PC can be removed. However, it can still be used as a terminal for reading or changing variables during normal operation of synchronous machine.

The basic menu for the synchronous machine model is shown in Figure 11.1. It presents the options the user has to set up and load the program for real time simulation.

Activities 1 to 3 allow the user to enter parameters for the model. Activity 4 executes HIDRAW graphical programming language environment, in which the models of exciter, PSS, governor and turbine can be set up. Activity 5 generates the complete code that will be loaded by activity 6 to the model hardware. Activity 7 can be used during simulation, if the user wants to monitor or change variables.

The set-up values for one of the AC generators are presented in section 11.2.9.

In order to find out adjustment faults, standard tests of the AC generator follow the set-up. Another reason for making the tests is to be able to prove that the AC generator is working in a correct way.

Open circuit test is made in order to check the d-axis transient open circuit time constant T_{d0} . Short circuit test is made in order to check the reactances and time constants of the model. The routines are described in [6].

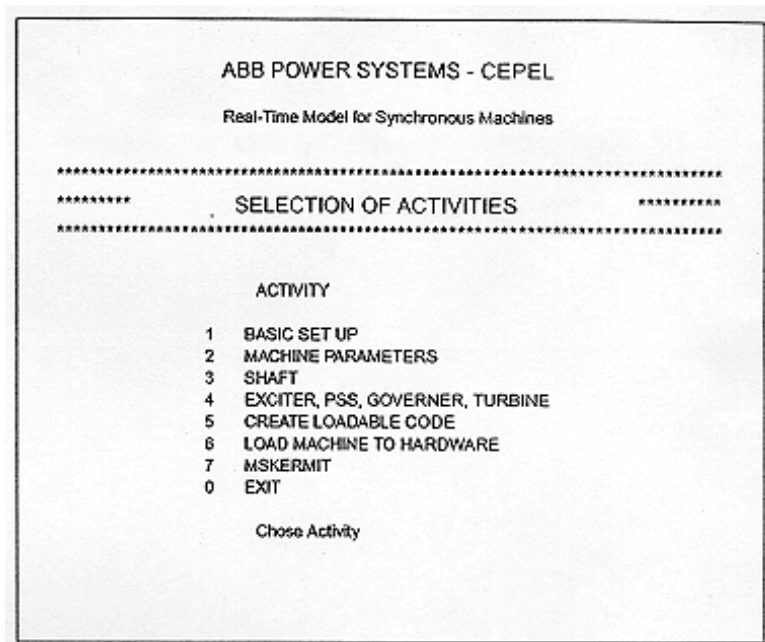


Figure 11.1 Basic menu for the synchronous machine model

After tests, the values of time constants and reactances are compared with set-up values and with simulation results obtained in EMTDC. Then the proper AC generator set-up is verified.

11.2.2 AC filters and PLC filters

The set-up of AC filters and PLC filters was verified after performing tests using frequency scanning. Each filter (the 25th and 41st harmonic filters (floating neutral point) and the 21st harmonic filter (grounded neutral point)) was tested separately sweeping the voltage in frequency range from 0 up to 10000 Hz into each separate phase. The proper tuning of the filters was verified.

11.2.3 DC cables, DC filters

The models of DC cables and DC filters were tested also using frequency scanning. The proper set-up of DC filters was verified by their tuning.. The DC cables representation was checked measuring impedance under four different circumstances: 1) short circuit pole mode, 2) open circuit pole mode, 3) short circuit ground mode, 4) open circuit ground mode. These frequency scanning results were compared with the simulation results obtained with EMTDC for verification of proper set-up.

11.2.4 Measurements

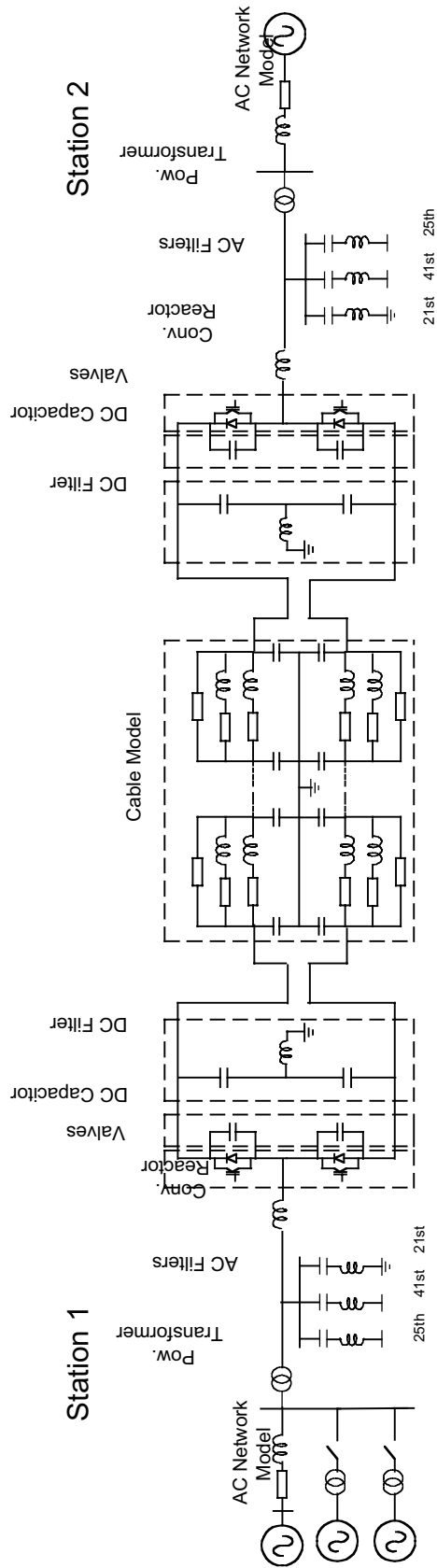
All measurements are documented and their correct action has to be verified.

11.2.5 Valves

Valve model was mounted and documented, and it was tested in blocked condition. In blocked condition the model acts as a diode rectifier and rectifies AC input voltage into DC output voltage.

11.2.6 Simulator Model

HVDC Light_B Real Time Analogue Simulator Model

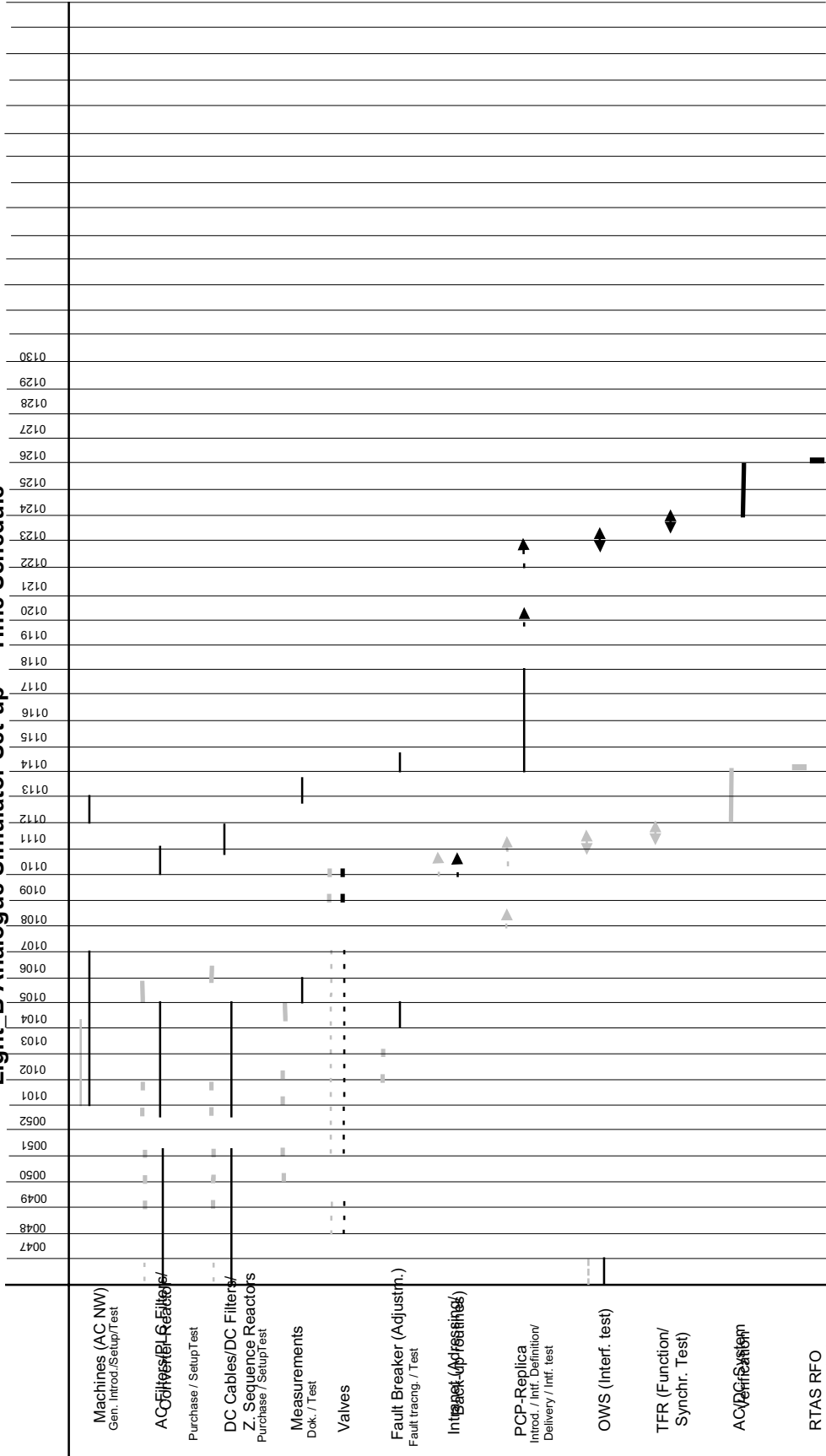


The PLC/RI filters and DC smoothing reactors are not shown above. Their details are given in the respective documentation

11.2.7 Time schedule

(Rev 01:01.03.20)

Light B Analogue Simulator Set-up - Time Schedule



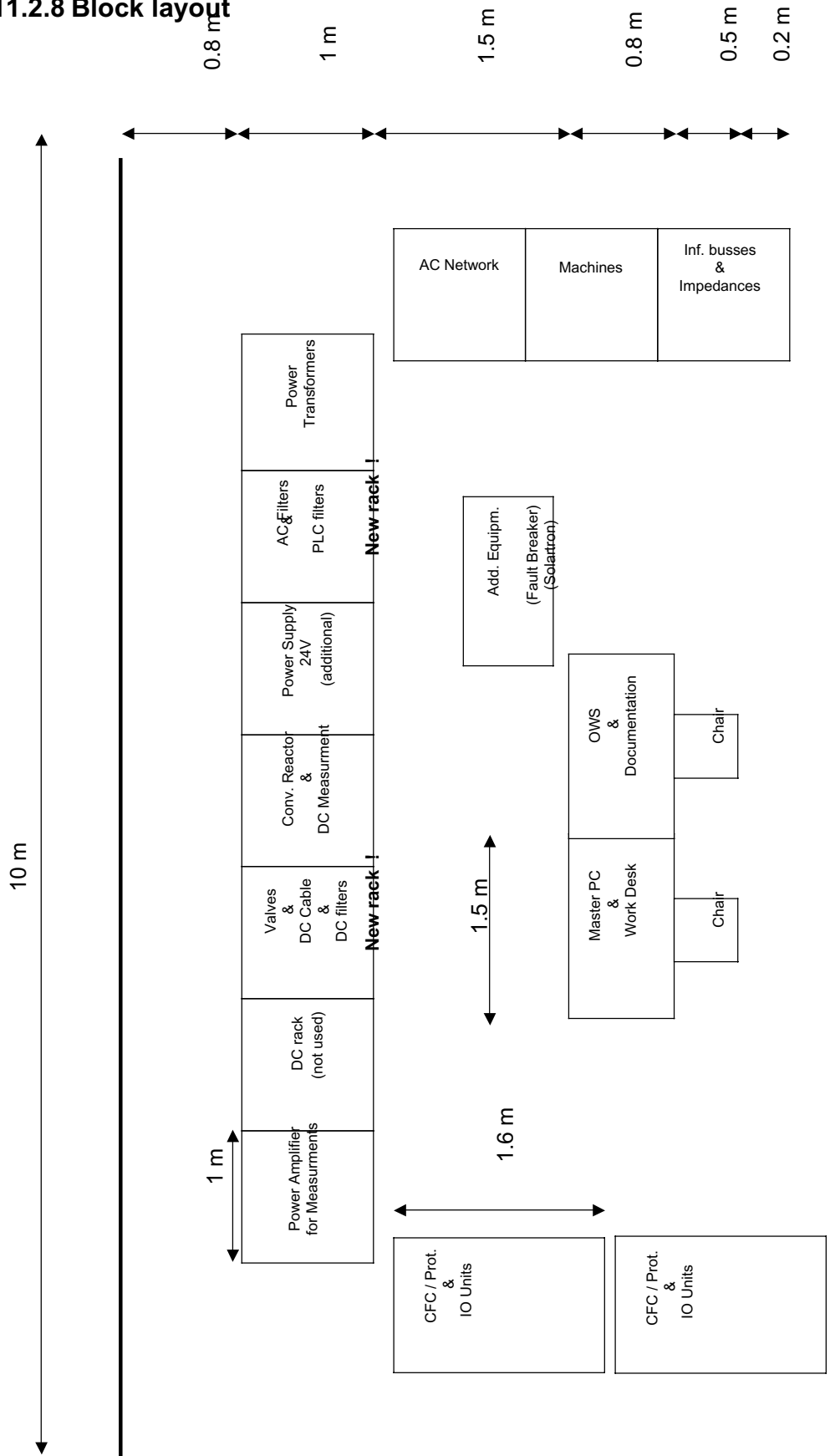
01:099 : Main circuit (except valves) available
01:109 : Tested Valve cubicles available
01:110 : Tested PCP cubicles available
01:110 : OWS Software available

01:107 : Main circuit (except valves) available
01:109 : Tested Valve cubicles available
01:110 : Tested PCP cubicles available
01:110 : OWS Software available

01:115 : Main circuit (except valves) available
01:110 : Tested Valve models available
01:121 : Tested PCP cubicles available
01:121 : OWS Software available

HVDC Light Real Time Analogue Simulator - Block Layout (Area: approx. (10x5) sq.m)

11.2.8 Block layout



11.2.9 Digital machine set-up values

S_n	99 MVA
U_n	13.8 kV
$S_{n\text{ sim}}$	$(99/346)*6 = 1.72$ VA
$U_{n\text{ sim}}$	$10 \sqrt{3}$ V
f_n	60 Hz
R_a	0.004 pu
X_a	0.148 pu
X_d	2.082 pu
X_q	1.97 pu
X_d	0.263 pu
X_q	0.43 pu
X_d	0.178 pu
X_q	0.16 pu
T_{do}	5.24 sec
T_{qo}	0.45 sec
T_{do}	0.023 sec
T_{qo}	0.054 sec
R_o	0 pu
X_o	0 pu
X_T	0.124 pu
R_T	0 pu
H	6.2 MWs/MVA